Cardiovascular Toxicology
https://doi.org/10.1007/s12012-020-09576-4

Involvement of ROS/NLRP3 Inflammasome Signaling Pathway in Doxorubicin-Induced Cardiotoxicity

Shanshan Wei[1,2] · Wanjun Ma[1,2] · Xiaohui Li[3] · Chuanhao Jiang[4] · Taoli Sun[5] · Yuanjian Li[3] · Bikui Zhang[1,2] · Wenqun Li[1,2]

Abstract

Doxorubicin (Dox) is widely used in cancer therapy, but the clinical application is limited by its cardiotoxicity. The underlying mechanism of Dox-induced cardiotoxicity remains unclear. Present study aimed to evaluate the role of NLRP3 inflammasome in Dox-induced cardiotoxicity. The NLRP3 inflammasome was activated in the myocardium of Dox-treating (5 mg/kg, once every other day, cumulative dosage to 15 mg/kg and sacrificed after 2 days of last Dox injection) C57BL/6 mice as shown by the up-regulation of NLRP3 and Caspase-1 p20. Dox (1 μM for 48 h) induced the apoptosis of H9c2 cells and primary cardiomyocytes concomitantly with up-regulation of NLRP3, ASC and Caspase-1 p20 expressions, as well as the increased IL-1β secretion, suggesting the activation of NLRP3 inflammasome. These effects of Dox on H9c2 cells and primary cardiomyocytes can be reversed by MCC950, a specific inhibitor of NLRP3. In view of the key role of ROS on the Dox-induced cardiotoxicity, the relationship between ROS and NLRP3 was further investigated. The ROS level was increased in myocardium, H9c2 cells and primary cardiomyocytes after treating with Dox. Decreasing ROS level by NAC can inhibit the NLRP3 inflammasome activation, secretion of IL-1β and apoptosis in Dox-treating H9c2 cells and primary cardiomyocytes. Collectively, this study reveals a crucial role of ROS/NLRP3-associated inflammasome activation in Dox-induced cardiotoxicity, and NLRP3 inflammasome may represent a new therapeutic target for Dox-induced cardiotoxicity.

Handling Editor: Yu-Ming Kang.

Shanshan Wei and Wanjun Ma contributed equally to this work.

✉ Bikui Zhang
505995@csu.edu.cn

✉ Wenqun Li
liwq1204@csu.edu.cn

[1] Department of Pharmacy, The Second Xiangya Hospital, Central South University, Changsha 410011, Hunan, China

[2] Institute of Clinical Pharmacy, Central South University, Changsha 410011, Hunan, China

[3] Department of Pharmacology, Xiangya School of Pharmaceutical Sciences, Central South University, Changsha 410008, Hunan, China

[4] Department of Laboratory Medicine, The Second Xiangya Hospital, Central South University, Changsha 410011, Hunan, China

[5] Key Laboratory Breeding Base of Hu'nan Oriented Fundamental and Applied Research of Innovative Pharmaceutics, College of Pharmacy, Changsha Medical University, Changsha 410219, Hunan, China

Published online: 30 June 2020

Graphic Abstract

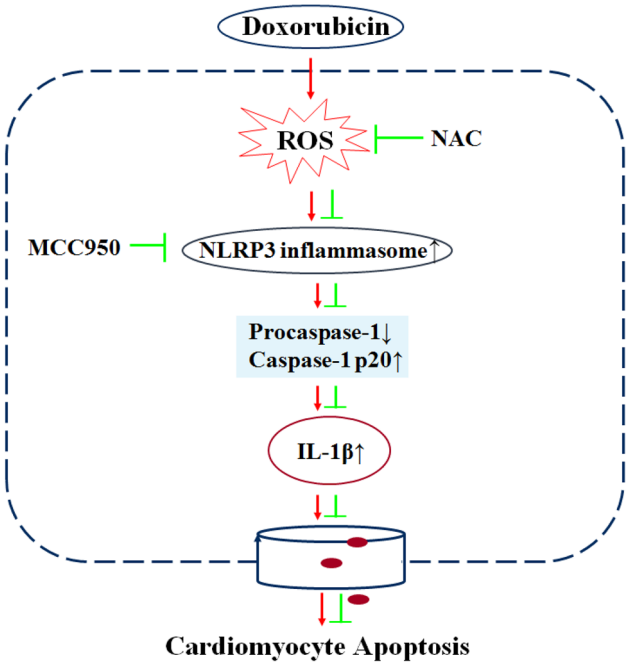

Keywords Doxorubicin · Cardiomyocyte · Apoptosis · NLRP3 inflammasome · ROS

Introduction

Doxorubicin (Dox) is the first anthracycline discovered in the 1960s, and it is now widely utilized in the therapy of solid and hematological malignancies [1]. However, the clinical application is limited by its side effects, especially dose-limiting cardiotoxicity [2]. Clinical studies indicate that more than 10–21% of patients occur acute cardiotoxicity within days after Dox administration, which predicts poor outcomes [3]. Chronic Dox-induced cardiotoxicity is less frequent but dose-dependent with a much higher incidence when exceeds the cumulative dosage of 400–700 mg/m^2 for adults and 300 mg/m^2 in the cases of children. The chronic cardiotoxicity commonly is detected years after therapeutic exposure, and typically manifests as an arrhythmia, cardiomyopathy, left ventricular dysfunction often associated with the clinical syndrome of heart failure [4]. Emerging studies proposed the indispensable role of cardiomyocyte apoptosis in Dox-induced cardiotoxicity [5], but the underlying mechanism hasn't yet fully elucidated.

Inflammasomes are cytosolic multiprotein complexes that cause the release of biologically active interleukin-1β (IL-1β). The best characterized inflammasome is the NLRP3 (Nod-like receptor protein 3) inflammasome [6]. Activation of NLRP3 inflammasome is initiated as assembly of NLRP3, apoptosis-associated speck-like protein containing a caspase recruitment domain (ASC) and Pro-caspase 1, leading to autocleavage of Pro-caspase 1 into active Caspase-1 heterodimers comprised of p10 and p20. Finally, active Caspase-1 cleaves pro-IL-1β into IL-1β that is released outside the cell to mediate inflammatory response [7]. Previous studies related to NLRP3 inflammasomes are focused on the immune response [8]. Recently, increased evidences found that NLRP3 inflammasome played a key role in cardiovascular disease [9]. It has been reported that the NLRP3 inflammasome contributes significantly to the pathological process of cardiac ischemia/reperfusion (I/R) injury [10], atherosclerosis [11] and other non-ischemic cardiac diseases [12]. In atherosclerosis and diabetic cardiomyopathy models, silencing NLRP3 or other inflammasome components could delay the deterioration and display overall beneficial effects [11, 12]. These studies triggered us to investigate the role of NLRP3 inflammasome in Dox-induced cardiotoxicity.

Our preliminary experiment indicated the activation of NLRP3 inflammasome in the myocardium of Dox-treating mice, which allowed us to explore the role of NLRP3 inflammasome in Dox-induced cardiomyocyte apoptosis. Additionally, reactive oxygen species (ROS) has been identified as an important NLRP3 inflammasome activator in cardiac diseases [13], and Dox-evoked ROS overproduction can elicit massive cardiomyocyte apoptosis in cardiotoxicity [14]. Therefore, this study further determined the relationship

between ROS and NLRP3 inflammasome in Dox-induced cardiotoxicity.

Materials and Methods

Animals and Procedures

Healthy C57BL/6 male mice (6–8 weeks-old, 20–25 g) were provided by Laboratory Animal Center, Xiangya School of Medicine, Central South University (Changsha, China). All the animals were housed at room temperature (20–24 °C), relative humidity (50–60%) under a 12 h light–dark cycle and with unrestricted access to water and fodder. All experiments were conducted according to the National Institutes of Health Guide (NIH publications No. 8023) for the Care and Use of Laboratory Animals, and approved by the Medicine Animal Welfare Committee of Xiangya School of Medicine (SYXK-2015/0017).

The mice were separated into two groups randomly and equally ($n=6$), for the Dox group, Dox hydrochloride Injection (Zhejiang Hisun Pharmaceutical co. LTD; Zhejiang, China) was dissolved in saline and intraperitoneal injected in mice (5 mg/kg, once every other day, cumulative dosage to 15 mg/kg) and the control group was given a considerable dose of saline. After 2 days of last Dox injection, all mice were anaesthetized with pentobarbital sodium and the blood and heart samples were collected immediately.

H9c2 Cell Culture

The H9c2 cells were obtained from American Type Culture Collection (Rockville, MD, USA) and maintained in Dulbecco's modified Eagle's medium F12 (HyClone, Logan, UT, USA) supplemented with 10% fetal bovine serum (FBS; Biological Industries, Israel), 100 units/mL of penicillin and 100 ug/mL streptomycin (Gibco Invitrogen, CA, USA) in a humidified atmosphere with 5% CO_2 at 37 °C.

Primary Cardiomyocytes Extract and Culture

Primary cardiomyocytes were isolated from the heart of neonatal male Sprague–Dawley rats (1–2 days old) through enzyme digestion in according to our previous study [15]. Myocardial tissue was cut into pieces with scissors, and then digested with deoxyribonuclease I (Sigma-Aldrich, USA) and trypsin (Gibco Invitrogen, CA, USA). The digestive enzyme mixture (1: 100) was placed in thermostatic bath at 37 °C for 8 min, and supernatant was collected and combined with FBS, then this process was repeated for 5 times. To collect cells, the combined supernatant was centrifuged (1000 rpm, 15 min) then resuspended in Dulbecco's modified Eagle's medium (Gibco Invitrogen, CA, USA) containing antibiotics (100 units/mL of penicillin and 100 ug/mL streptomycin) and 20% fetal bovine serum (20% FBS DMEM). Cells were filtered through 100 μm mesh and plated on culture dish for 90 min. The supernatant were centrifuged (1000 rpm, 5 min) to collect cardiomyocytes, which then resuspended in 20% FBS DMEM containing 0.1 mM 5-Bromo-2-deoxyuridine (Sigma-Aldrich, USA) and used for the following experiments.

Cell Viability Assay

The primary cardiomyocytes were cultured in 96-well plates and treated with doxorubicin or inhibitor for 48 h. Then 100 μl of medium containing 15% MTS (cellTiter 96®AQueous one solution cell proliferation assay kit, Promega, USA) was added to each well, and OD values were measured at 492 nm after 1 h of incubation at 37 °C using a microplate reader (BioTek, Winooski, VT, USA).

Biochemical Analysis

The solidified blood samples collected from animals were centrifuged at 4000 rpm in 4 °C for 15 min to obtain serum. The serum biochemical parameters including cardiac troponin T (cTnT), Creatine Kinase (CK), CK-MB, lactate dehydrogenase (LDH), as well as the supernatant IL-1β and LDH harvested from cultured H9c2 cells and primary cardiomyocytes after treatment were analyzed by using kits with an automatic biochemical analyzer (Abbott Pharmaceutical Co., Ltd., Lake Bluff, IL, USA). The experiments were performed according to the manufacturers' instructions.

Histopathological Analysis

Hearts were fixed with 4% paraformaldehyde and embedded in paraffin. Hematoxylin–eosin (HE) staining, wheat germ agglutinin (WGA) staining and TdT-mediated dUTP Nick-End Labeling (TUNEL) kit assay in heart section were conducted according to the manufacturer's instructions as our previous study [16].

Immunohistochemistry

Paraffin-embedded heart section (5 μm) was prepared. Then, sections were incubated with anti-NLRP3 antibody (1:100 dilution, AdipoGen; San Diego, USA) at 4 °C overnight. Subsequently, the sections were incubated with horseradish peroxidase (HRP)-conjugated secondary antibody for 30 min at room temperature. Fresh 3, 30-diaminobenzidine (DAB) solution was added to the sections, and the sections were counterstained with hematoxylin. Images were captured under microscopy.

Assessment of ROS Generation

The fluorescent probe dihydroethidium (DHE; Beyotime, Shanghai, China) was used to monitor intracellular ROS levels. Intracellular DHE is oxidized to ethidium, which binds to DNA and stains the nuclei bright fluorescent red. The detection of ROS level in heart section, H9c2 cells and primary cardiomyocytes were conducted according to the manufacturer's instructions as our previous study [17].

Western Blot Analysis

Fresh animal hearts, H9c2 cells and primary cardiomyocytes were lysed in RIPA buffer (containing 1% PMSF) (BOSTER Biological Technology; Wuhan, China). Proteins were separated by sodium dodecyl sulfate–polyacrylamide gel electrophoresis (SDS-PAGE) using a 10% gradient gel and transferred onto 0.45 μm polyvinylidene fluoride (PVDF) membranes. The membranes were blocked with 5% non-fat milk and incubated with anti-NLRP3 (AdipoGen; San Diego, USA), anti-ASC (Abcam; Cambridge, UK), anti-Procaspase 1, anti-Bax and anti-GAPDH (Abcam; Cambridge, UK), anti-caspase1 p20 (Affinity Biosciences. OH. USA), anti-Bcl-2 (ProteinTech; Chicago, USA) antibodies at 4 ℃ overnight. The membranes were then incubated with HRP-conjugated anti-mouse or anti-rabbit IgGs at room temperature for 1 h. The chemiluminescence signals were detected with the BeyoECL plus kit (Beyotime; Shanghai, China). ImageJ 1.43 (National Institutes of Health) was used for densitometric analysis.

Flow Cytometric Analysis

Flow cytometric analysis was performed according to the manufacturers' instructions (BD Biosciences; New York, USA). Cells were washed twice with cold phosphate buffered saline (PBS) and then resuspended in 1 × binding buffer at a concentration of 1×10^6 cells/ml. A total of 100 μl of the solution (1×10^5 cells) was transferred to a 5 ml culture tube. After adding 5 μl FITC Annexin V and 5 μl propidium iodide (PI), the cells were gently vortexed and incubated for 15 min at room temperature (25 °C) in the dark, followed by the addition of 400 μl of 1 × binding buffer to each tube. Analysis by flow cytometry was performed within 1 h.

Hoechst Staining

Hoechst 33342 is a blue fluorescent dye that can penetrate the cell membrane and it can emit blue fluorescence after binds with double-stranded DNA. After treatment, cells were washed by PBS then fixed with 4% paraformaldehyde for 15 min, cells were washed by PBS once more and incubated with Hoechst 33342 (5 μg/ml, Beyotime; Shanghai, China) for 20 min according to the manufacturer's instructions. Fluorescence was observed under the fluorescence microscope and representative images were captured.

Statistical Analysis

The results were presented as means ± S.E.M. Two-tailed Student's t-test was used for data comparison of two groups with normal distribution; one-way ANOVA and Student–Newman–Keuls test were used for multiple comparisons. Results were considered statistically significant when $P < 0.05$.

Results

Dox-Induced Cardiotoxicity in C57BL/6 Mice

The Dox-induced cardiotoxicity model was established via intraperitoneal administration of Dox (15 mg/kg) in C57BL/6 mice. As shown in Fig. 1, after administration of Dox, the serum concentrations of cTnT (Fig. 1a), CK (Fig. 1b), CK-MB (Fig. 1c) and LDH (Fig. 1d), which acted as the bio-marker of cardiac injury, were significantly increased. Moreover, HE staining was conducted in myocardium to observe the effect of Dox on cardiac structure. The Dox group demonstrated obvious cardiac injury (caryolysis, disorganization of the muscle fibers and interstitial edema) compared with the control group (Fig. 1e). The result of WGA staining indicated the enlargement of cardiomyocyte size induced by Dox (Fig. 1f). These results demonstrated that the Dox-induced cardiotoxicity model was successfully established in mice.

Dox Induced the Overproduction of ROS and Cardiomyocyte Apoptosis in Mice

Since the production of ROS and apoptosis play a central role in the Dox-induced cardiotoxicity, DHE and TUNEL staining were used to evaluate whether Dox increased the ROS level and cardiomyocyte apoptosis in our model. The representative fluorescent images revealed that treatment with Dox increased red fluorescence, suggested the overproduction of ROS in the heart (Fig. 2a). Additionally, increased percentage of TUNEL staining-positive cells was observed in Dox-treated mice, indicating the apoptosis of cardiomyocyte (Fig. 2b). The up-regulation of pro-apoptosis protein Bax and the down-regulation of anti-apoptosis

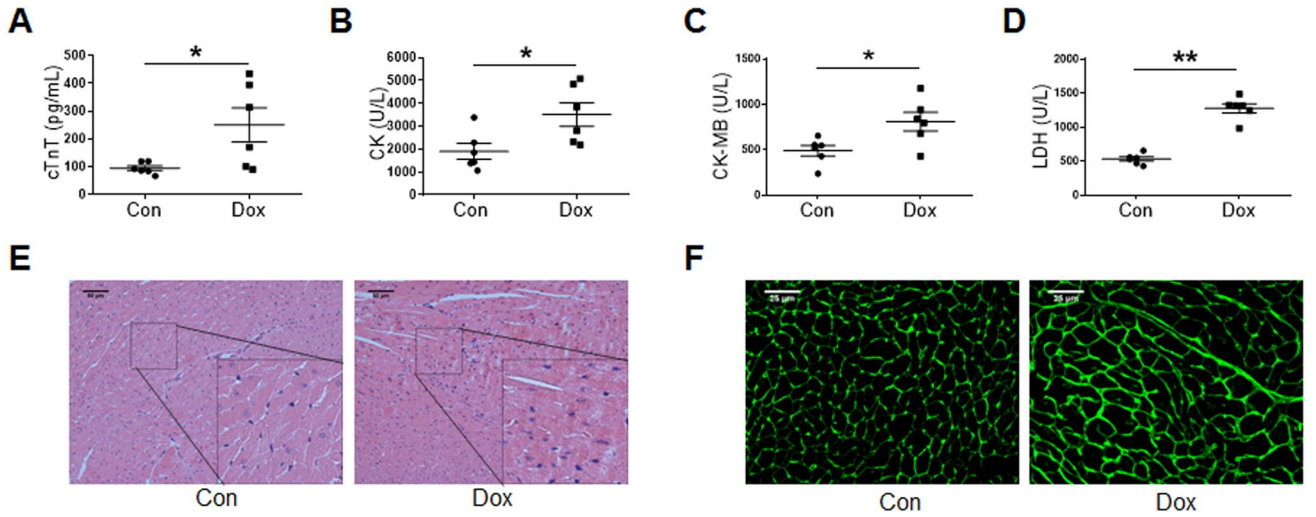

Fig. 1 Cardiotoxicity induced by Dox in C57BL/6 mice. Serum cTnT (**a**), CK (**b**), CK-MB (**c**) LDH (**d**) were measured by using kits with an automatic biochemical analyzer. **e** Representative images of HE staining. **f** Wheat germ agglutinin (WGA) staining of left ventricular tissue for determination of cardiomyocytes cross-sectional area, scale bar = 25 μm. Data are mean ± S.E.M. n = 6 mice per group. *$P < 0.05$, **$P < 0.01$ vs. Con

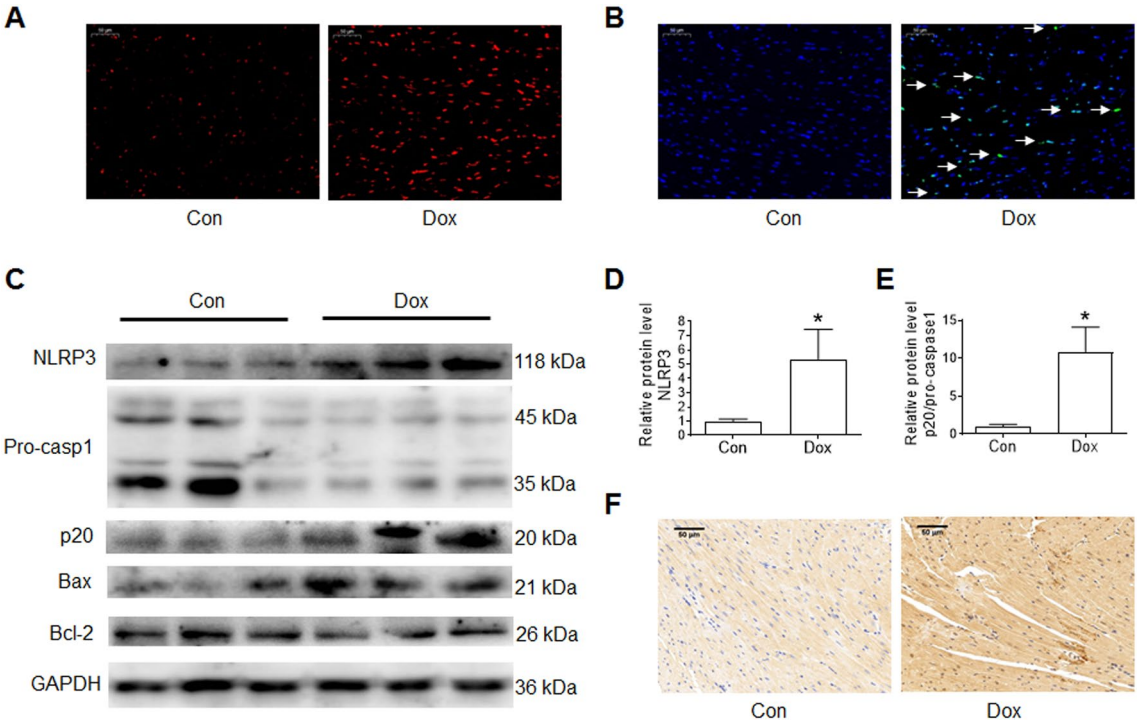

Fig. 2 Dox-induced ROS overproduction, cardiomyocytes apoptosis and activation of NLRP3 inflammasome in C57BL/6 mice. **a** ROS level in myocardium was determined by DHE staining, scale bar = 50 μm. **b** Representative images of TUNEL staining in myocardium, apoptotic cardiomyocytes nuclei appear green fluorescence and normal nuclei appear blue fluorescence, the white array indicated the apoptotic cardiomyocytes, scale bar = 50 μm. **c**–**e** The protein expressions of NLRP3, Pro-caspase 1(Pro-casp1), Caspase-1 p20 (p20), Bax and Bcl-2 in myocardium were measured by western blot, GAPDH served as loading control. **f** Representative images of NLRP3 immunohistochemistry in myocardium, scale bar = 50 μm. Data are mean ± S.E.M. $n = 6$ mice per group. *$P < 0.05$ vs. Con

protein Bcl-2 also identified the cardiomyocyte apoptosis in Dox-treating mice (Fig. 2c).

NLRP3 Inflammasome was Activated in Dox-Induced Cardiotoxicity of Mice

To further explore whether the activation of NLRP3 inflammasome was involved in the Dox-induced cardiotoxicity, protein expressions of inflammasome in the myocardium were determined. As shown in Fig. 2c, d and f, the results of immunohistochemistry and western blot all showed that NLRP3, the upstream initiator of NLRP3 inflammasome, was up-regulated in the myocardium of mice treated with Dox. Besides, the expression of Pro-caspase 1 was decreased and correspondingly, the expression of Caspase-1 p20 was significantly increased in Dox-treated group, which indicated the activation of Caspase-1 (Fig. 2c, f). Collectively, these results implied that the activation of NLRP3 inflammasome was concerned to the cardiotoxicity induced by Dox.

Inhibition of NLRP3 Suppressed the Dox-Induced NLRP3 Inflammasome Activation and Apoptosis in H9c2 Cells

In order to further confirm the key role of NLRP3 inflammasome in Dox-induced cardiotoxicity, the in vitro experiment were performed in H9c2 cells. In consistent with the in vivo results, NLRP3 inflammasome was activated in Dox-treating H9c2 cells as indicated by up-regulation of NLRP3 and Caspase-1 p20, as well as the increased secretion of IL-1β (Fig. 3a–e). Moreover, the H9c2 cells treating with Dox exhibited increased percentage of Hoechst staining-positive cells (Fig. 4a, b), Annexin V-FITC/PI double staining showed that Dox induced approximately 60% H9c2 cells apoptosis (Fig. 4c, d). Up-regulation of Bax and down-regulation of Bcl-2 (Fig. 4e, f), also suggested apoptosis induced by Dox, and increased LDH level in supernatants indicated the injury induced by Dox in H9c2 cells (Fig. 3f). To determine the role of NLRP3 inflammasome in Dox-induced H9c2 cells apoptosis, pretreatment of MCC950, a specific NLRP3 inhibitor, was conducted in Dox-treating H9c2 cells. The results showed that Dox-induced NLRP3 inflammasome activation and apoptosis in H9c2 cells were reversed by MCC950 (Fig. 4a–f), suggested that inhibition

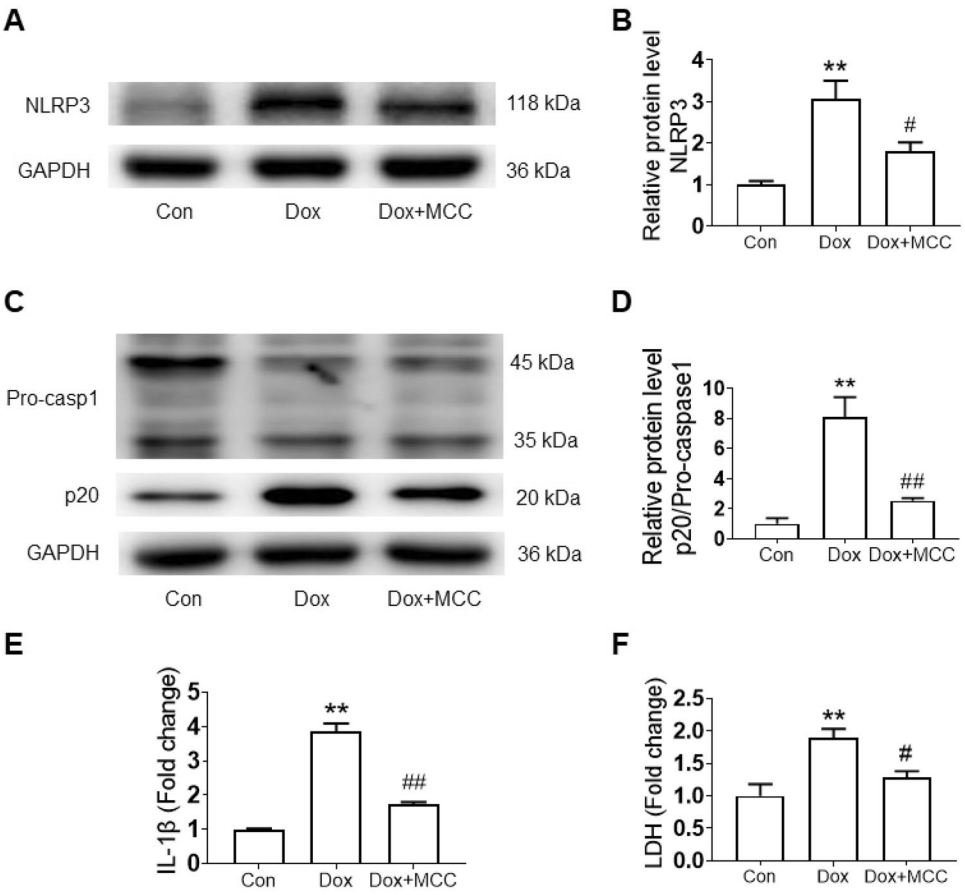

Fig. 3 Inhibition of NLRP3 suppressed NLRP3 inflammasome activation induced by Dox in H9c2 cells. H9c2 cells were pretreated with NLRP3 inhibitor MCC950 (MCC, 10 μM) for 1 h and then incubated with 1 μM Dox for 48 h, 0 μM Dox treatment was used as Control. **a**–**d** The protein expression of NLRP3, Pro-caspase 1 and Caspase-1 p20 were determined by western blot, GAPDH served as loading control. **e**, **f** The levels of IL-1β (**e**) and LDH (**f**) in the supernatant were measured by using kits with an automatic biochemical analyzer. Data are mean ± S.E.M. $n = 3$. $^{**}P < 0.01$ vs. Con. $^{\#}P < 0.05$, $^{\#\#}P < 0.01$ vs. Dox

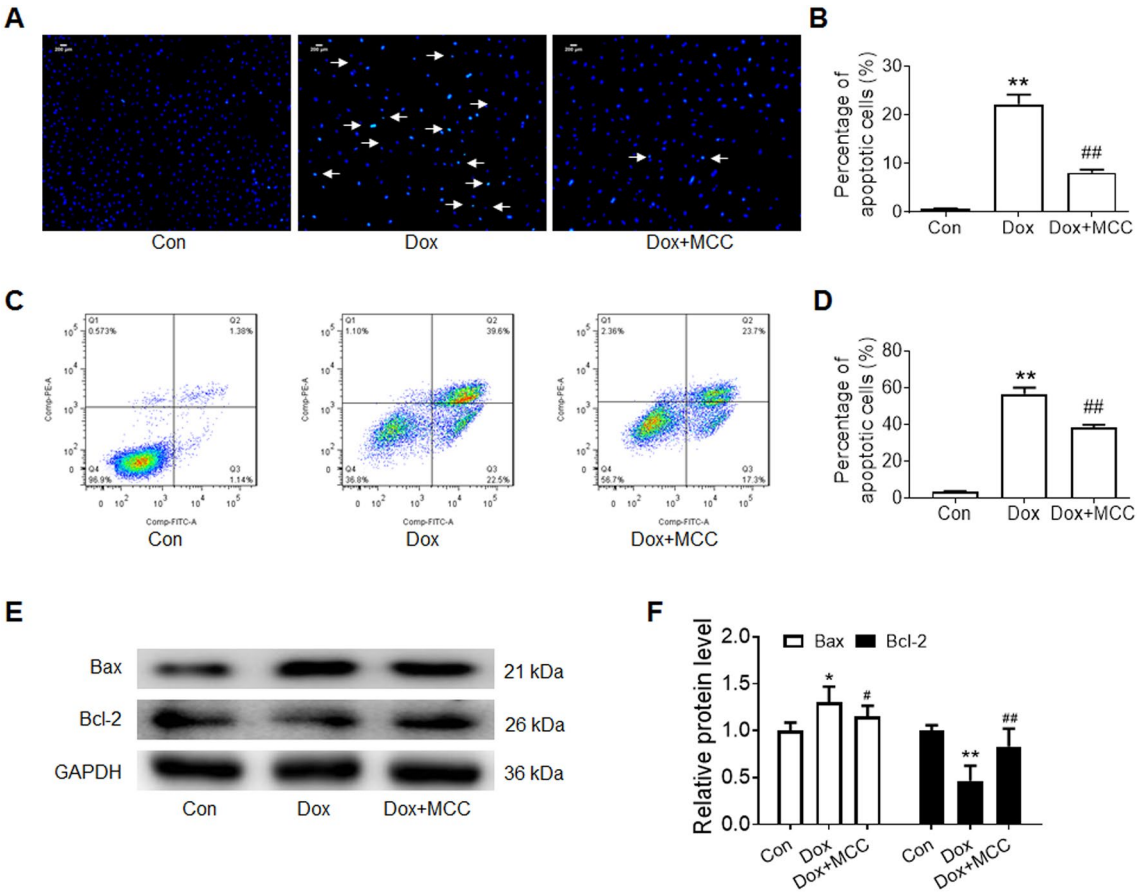

Fig. 4 Inhibition of NLRP3 suppressed Dox-induced apoptosis in H9c2 cells. **a**, **b** Representative images of Hoechst 33342 staining and statistical analysis, scale bar = 200 μm. **c**, **d** Representative flow cytometry scatter plots of Annexin V-fluorescein isothiocyanate (FITC)/Propidium iodide staining and statistical analysis. **e**, **f** The protein expression of Bax and Bcl-2 were determined by western blot, GAPDH served as loading control. Data are mean ± S.E.M. $n = 3$. $^{*}P < 0.05$, $^{**}P < 0.01$ vs. Con. $^{\#}P < 0.05$, $^{\#\#}P < 0.01$ vs. Dox

of NLRP3 suppressed the Dox-induced NLRP3 inflammasome activation and apoptosis in H9c2 cells.

Inhibition of NLRP3 Suppressed the Dox-Induced NLRP3 Inflammasome Activation and Apoptosis in Primary Cardiomyocytes

Because of that H9c2 cells can't fully show the phenotype of cardiomyocytes, we isolated and cultured the primary cardiomyocytes, and investigated the effect of NLRP3 inhibitor on the Dox-induced NLRP3 inflammasome activation and apoptosis. In consistent with the results obtained in H9c2 cells, NLRP3 inhibitor MCC950 could inhibit the Dox-induced NLRP3 inflammasome activation (Fig. 5a–c) in primary cardiomyocytes.

It is well known that cardiomyocytes act as terminally differentiated cells, have no proliferative ability. Therefore, the decreased cell viability also reflects the apoptosis of primary cardiomyocytes in addition to the LDH level, Hoechst staining. As shown in Fig. 5g, Dox decreased the cell viability, which was reversed by NLRP3 inhibitor MCC950. These results in Fig. 5d–g, collectively, suggested that inhibition of NLRP3 suppressed Dox-induced apoptosis in primary cardiomyocytes.

ROS Scavenger Suppressed the Dox-Induced NLRP3 Inflammasome Activation and Apoptosis in H9c2 Cells and Primary Cardiomyocytes

Our in vivo study has determined the overproduction of ROS in the heart of Dox-treating mice. The ROS acted as an important activator for NLRP3 inflammasome, therefore, which allowed us to investigate the relationship between ROS and NLRP3 inflammasome in Dox-induced cardiotoxicity. The DHE staining showed that Dox induced the ROS overproduction, while pretreatment of NAC, a ROS scavenger, can decrease the ROS level in Dox-treating H9c2 cells (Fig. 6a). Moreover, pretreatment of NAC can inhibit the up-regulation of NLRP3, ASC and Caspase-1

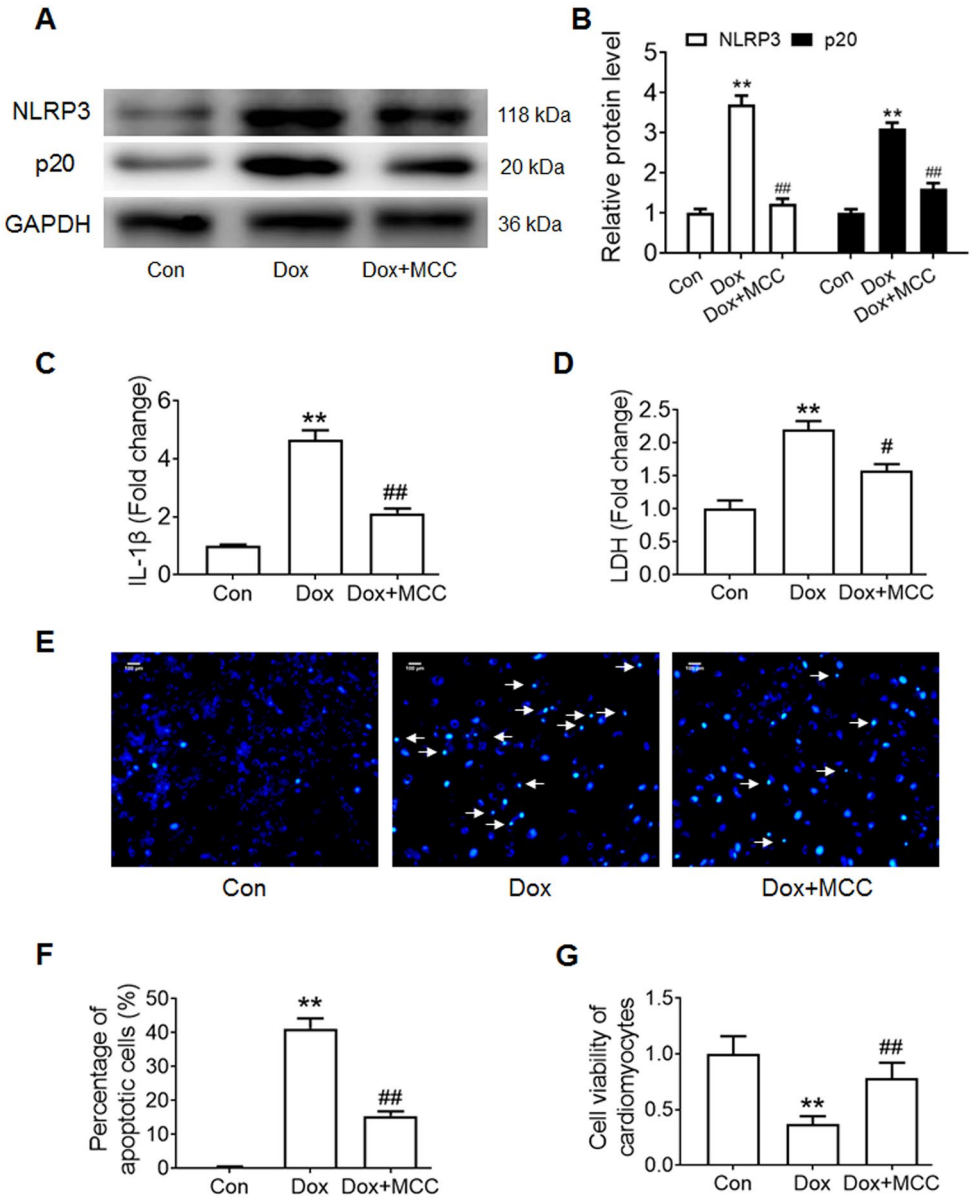

Fig. 5 Inhibition of NLRP3 suppressed Dox-induced NLRP3 inflammasome activation and apoptosis in primary cardiomyocytes. Primary cardiomyocytes were pretreated with MCC950 for 1 h and then incubated with 1 μM Dox for 48 h. **a**, **b** The protein expression of NLRP3 and Caspase-1 p20 were determined by western blot, GAPDH served as loading control. **c**, **d** The levels of IL-1β (**c**) and LDH (**d**) in the supernatant were measured by using kits with an automatic biochemical analyzer. **e**, **f** Representative images of Hoechst 33342 staining and statistical analysis, scale bar = 100 μm. **g** Cell viability was measured by CellTiter 96® AQueous One Solution Cell Proliferation Assay. Data are mean ± S.E.M. $n = 3$. $^{**}P < 0.01$ vs. Con. $^{\#}P < 0.05$, $^{\#\#}P < 0.01$ vs. Dox

p20 expression, as well as the IL-1β, suggesting that inhibition of ROS suppressed the Dox-induced NLRP3 inflammasome activation in H9c2 cells (Fig. 6b–f). Decrease of ROS also suppressed the cell apoptosis and injury induced by Dox. As shown by Fig. 7a–f, the increased percentage of Hoechst staining-positive cells (Fig. 7a, b), up-regulation of Bax and down-regulation of Bcl-2 induced by Dox can be inhibited by NAC (Fig. 7e, f). The results of Annexin V-FITC/PI double staining and LDH level in supernatants further identified this speculation (Figs. 6g, 7c, d). Moreover, in consistent with the results obtained in H9c2 cells, ROS scavenger suppressed the Dox-induced NLRP3 inflammasome activation in primary cardiomyocytes (Fig. 8a–h).

Discussion

Inflammation is originally recognized as the response to infection, which is triggered by innate immune system, such as neutrophils and macrophages [8]. However, increasing evidence indicates that inflammatory responses also occur in the absence of infection, and is named "sterile inflammation". The sterile inflammation has been found in multiple diseases including gout, type 2 diabetes mellitus, Alzheimer's disease et al. [18]. Although complex underlying mechanisms are involved in sterile inflammation, "inflammasomes" has been defined as playing crucial role in the processes of sterile inflammation [6]. Inflammasomes, a large multiple cytoplasmic protein complex served as platforms for Caspase-1 activation, are typically contain one

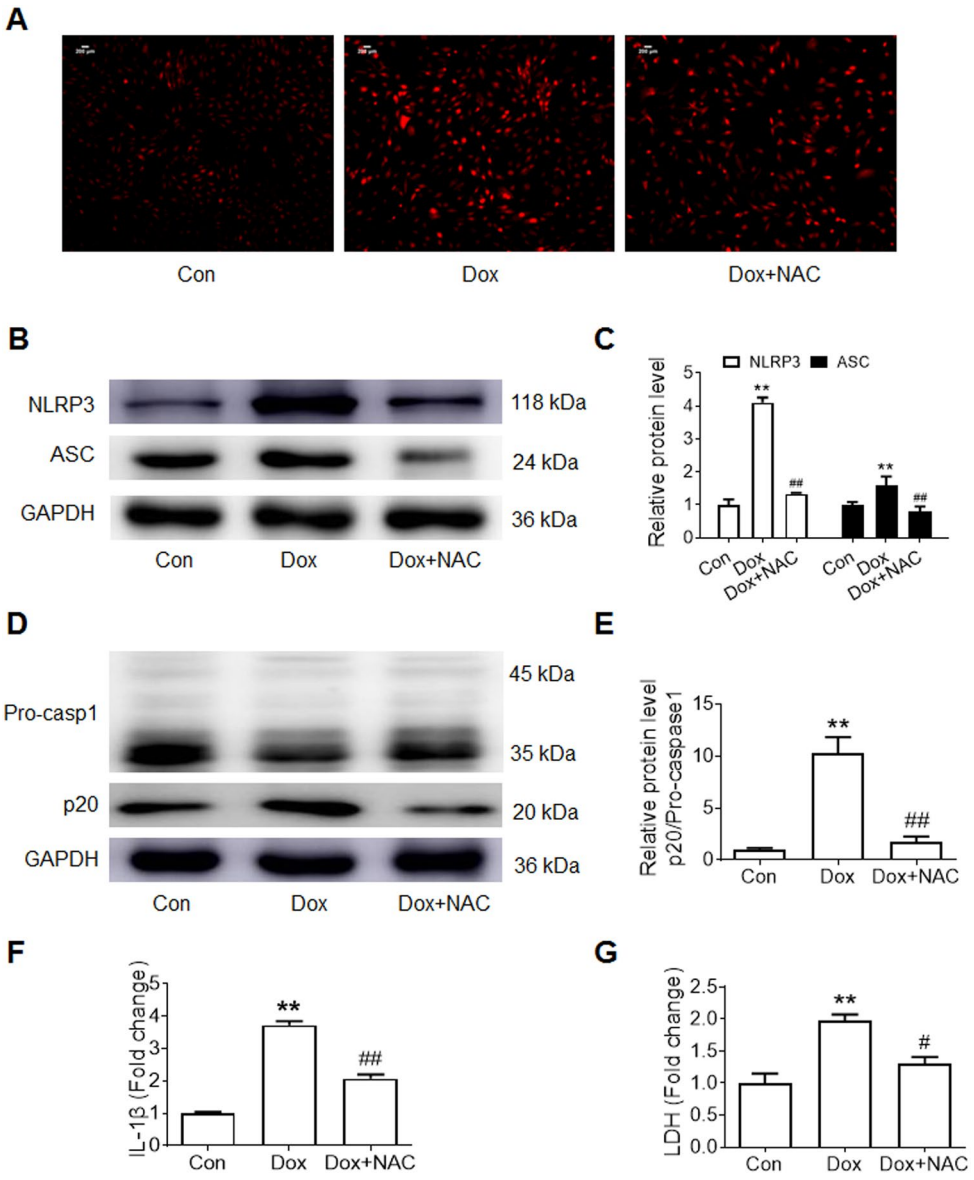

Fig. 6 ROS scavenger suppressed NLRP3 inflammasome activation induced by Dox in H9c2 cells. H9c2 cells were pretreated with ROS scavenger *N*-acetylcysteine (NAC, 2 mM) for 1 h and were then incubated with 1 μM Dox for 48 h, 0 μM Dox treatment was used as Control. **a** ROS level was determined by DHE staining, scale bar = 200 μm. **b**–**e** The protein expression of NLRP3, ASC, Pro-caspase 1 and Caspase-1 p20 were determined by western blot, GAPDH served as loading control. **f**, **g** The levels of IL-1β (**f**) and LDH (**g**) in the supernatant were measured by using kits with an automatic biochemical analyzer. Data are mean ± S.E.M. $n = 3$. $^{**}P < 0.01$ vs. Con. $^{\#}P < 0.05$, $^{\#\#}P < 0.01$ vs. Dox

of the NLR family proteins, apoptosis-associated speck-like protein containing a caspase recruitment domain (ASC), and the cysteine protease Caspase-1 [7].

NLRs include NLRP1, NLRP3, NLRP6, NLRP7, NLRP12, and NLRC4, among them, the NLRP3 inflammasome is the most extensively studied and has been reported to recognize danger signals and trigger sterile inflammatory responses in various diseases [19]. For example, inhibition of NLRP3 by siRNA or specific inhibitor prevented inflammasome activation and cardiomyocyte death, resulting in ameliorating myocardial remodeling after myocardial infarction [20]. Moreover, ASC-KO or Caspase-1-KO mice exhibited a significant decline of inflammatory responses, and showed a significant reduction of infarct size and left ventricular dysfunction after myocardial infarction [21]. These studies suggested that NLRP3 inflammation is involved in mediating myocardial damage and repair. In present study, we established the model of Dox-induced cardiotoxicity in mice, and found that NLRP3 and Caspase-1 p20 were up-regulated in myocardium of Dox-treating mice, indicating the activation of NLRP3 inflammasome. This result allowed us to investigate the role of NLRP3 inflammasome in Dox-induced cardiotoxicity. Growing evidence supported the view that apoptotic death of cardiomyocytes acted as the main cause of Dox-induced cardiotoxicity [22]. Therefore, the role of NLRP3 inflammasome in Dox-induced cardiomyocytes apoptosis was determined. In consistent with the in vivo results, Dox induced the apoptosis of cardiomyocytes concomitantly with NLRP3 inflammasome activation, as shown by the up-regulation of NLRP3, ASC and Caspase-1 p20 expressions. Moreover, inhibition of NLRP3 suppressed the inflammasome activation, and reversed the

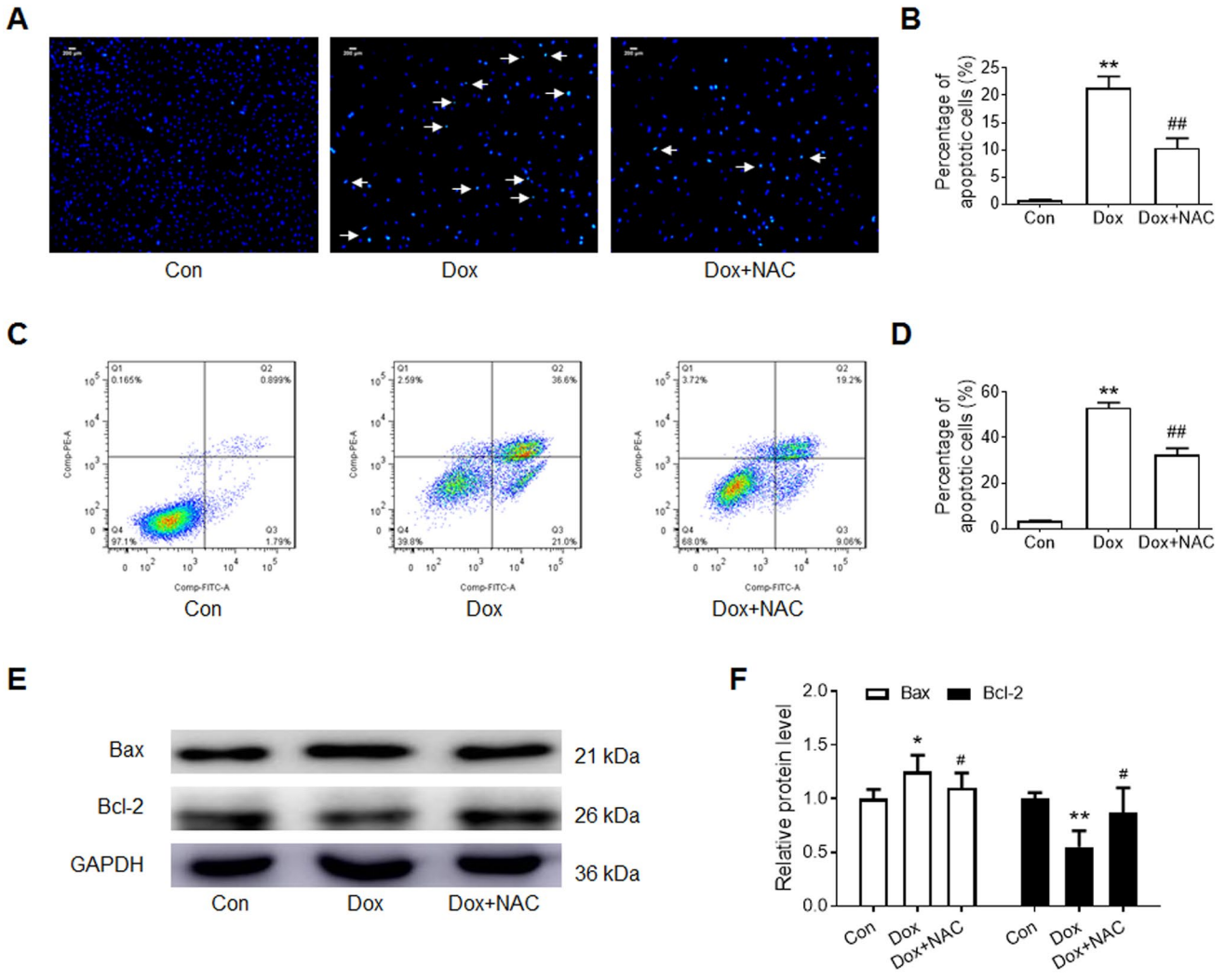

Fig. 7 ROS scavenger suppressed Dox-induced apoptosis in H9c2 cells. **a**, **b** Representative images of Hoechst 33342 staining and statistical analysis, scale bar = 200 μm. **c**, **d** Representative flow cytometry scatter plots of Annexin V-fluorescein isothiocyanate (FITC)/Propidium iodide staining and statistical analysis. **e**, **f** The protein expression of Bax and Bcl-2 were determined by western blot, GAPDH served as loading control. Data are mean ± S.E.M. $n = 3$. $^{*}P < 0.05$, $^{**}P < 0.01$ vs. Con. $^{\#}P < 0.05$, $^{\#\#}P < 0.01$ vs. Dox

Dox-induced cardiomyocytes apoptosis. These results suggested that the NLRP3 inflammasome mediated the Dox-induced cardiotoxicity.

The Caspase-1 activation in NLRP3 inflammasome cleaves pro-IL-1β and pro-IL-18 into the biologically active forms IL-1β and IL-18, finally initiating the sterile inflammatory disease [7]. An excessive inflammatory response has been observed in diversity cardiomyopathy [23]. Treatment with antibodies against IL-1β (canakimumab) and IL-6 (tocilizumab) leaded to significant cardioprotection effects. Neutralization of IL-1 reduced acute and chronic myocarditis in mice [24, 25]. These studies identified the central role of inflammatory response in the pathophysiology of cardiac damage, which was also verified in present study. The secretion of IL-1β was increased in Dox-treating cardiomyocytes concomitantly with NLRP3 inflammasome activation and cells apoptosis, while inhibition of NLRP3 can decrease the IL-1β secretion.

The NLRP3 inflammasome can be activated by diverse stimuli, and multiple molecular and cellular events, including ionic flux, mitochondrial dysfunction, and overproduction of ROS [26]. As the dynamic organ of human blood circulation, heart is rich in mitochondria, especially the cardiomyocytes. Compared with the number in other tissues, the number of mitochondria in cardiomyocytes was increased by 35–40%, that is why the Dox-induced toxicity priority for heart [27]. Present study was consistent with previous reported study, observed the overproduction of ROS in Dox-treating myocardium and cardiomyocytes. Considering the key roles of ROS/NLRP3 inflammasome activation

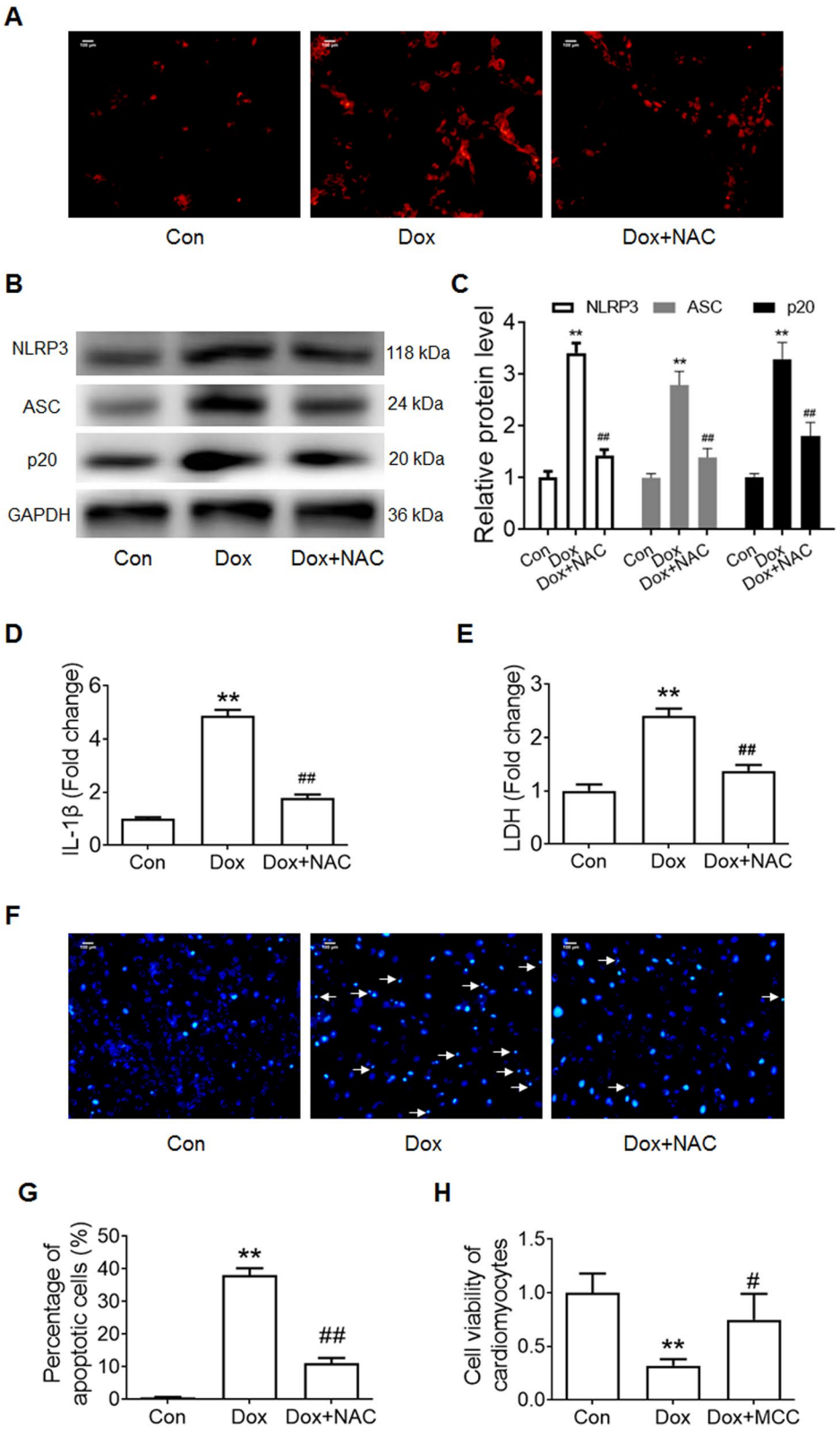

Fig. 8 ROS scavenger suppressed the Dox-induced NLRP3 inflammasome activation and apoptosis in primary cardiomyocytes. Primary cardiomyocytes were pretreated with NAC for 1 h and then incubated with 1 μM Dox for 48 h. **a** ROS level was determined by DHE staining, scale bar = 100 μm. **b**, **c** The protein expression of NLRP3, ASC and Caspase-1 p20 were determined by western blot, GAPDH served as loading control. **d**, **e** The levels of IL-1β (**d**) and LDH (**e**) in the supernatant were measured by using kits with an automatic biochemical analyzer. **f**, **g** Representative images of Hoechst 33342 staining and statistical analysis, scale bar = 100 μm. **h** Cell viability was measured by CellTiter 96® AQueous One Solution Cell Proliferation Assay. Data are mean ± S.E.M. $n = 3$. $^{**}P < 0.01$ vs. Con. $^{\#}P < 0.05$, $^{\#\#}P < 0.01$ vs. Dox

in LPS-ATP-induced endothelial cell pyroptosis [28], acute ozone-induced airway inflammation [29], and especially the Dox-induced renal tubule injury (30), present study further determined whether ROS acted as NLRP3 inflammasome activator in Dox-induced cardiotoxicity. We found that decreasing ROS level by NAC can inhibit the NLRP3

inflammasome activation, secretion of IL-1β and apoptosis in Dox-treating cardiomyocytes. These results suggested that the NLRP3 inflammasome activation in Dox-induced cardiotoxicity was regulated by the overproduction of ROS.

In summary, we found that NLRP3 inflammasome was activated in the myocardium and cardiomyocytes after treatment with Dox. Inhibition of NLRP3 reversed the Dox-induced cardiomyocytes apoptosis, and the activation of NLRP3 inflammasome was regulated by ROS. Based on the data described herein, present study determined the key role of ROS/NLRP3 inflammasome activation in Dox-induced cardiotoxicity. These findings may have important implications with respect to better understanding the mechanisms underlying Dox-induced cardiotoxicity.

Acknowledgements This work was supported by Grants of the National Natural Scientific Foundation of China (Nos. 81703518, 81973406, 81773734, 81701577), Hunan Provincial Natural Scientific Foundation (Nos. 2018JJ3571, 2019JJ50849, 2020JJ4823), Fundamental Research Funds for the Central Universities of Central South University (No. 2020zzts822), and Scientific Research Project of Hunan Provincial Health and Family Planning Commission (No. B20180253).

Compliance with Ethical Standards

Conflict of interest The authors declare that they have no conflicts of interest.

References

1. Cagel, M., Grotz, E., Bernabeu, E., Moretton, M. A., & Chiappetta, D. A. (2017). Doxorubicin: Nanotechnological overviews from bench to bedside. *Drug Discovery Today, 22*, 270–281.
2. Renu, K., Abilash, V. G., & Arunachalam, S. (2018). Molecular mechanism of doxorubicin-induced cardiomyopathy—An update. *European Journal of Pharmacology, 818*, 241–253.
3. Caram, M. E. V., Guo, C., Leja, M., Smerage, J., Henry, N. L., Giacherio, D., et al. (2015). Doxorubicin-induced cardiac dysfunction in unselected patients with a history of early-stage breast cancer. *Breast Cancer Research and Treatment, 152*, 163–172.
4. Xin, Y. F., Zhou, G. L., Shen, M., Chen, Y. X., Liu, S. P., Chen, G. C., et al. (2007). Angelica sinensis: A novel adjunct to prevent doxorubicin-induced chronic cardiotoxicity. *Basic & Clinical Pharmacology & Toxicology, 101*, 421–426.
5. Zhang, X., Hu, C., Kong, C. Y., Song, P., Wu, H. M., Xu, S. C., et al. (2020). FNDC5 alleviates oxidative stress and cardiomyocyte apoptosis in doxorubicin-induced cardiotoxicity via activating AKT. *Cell Death and Differentiation, 27*, 540–555.
6. Yu, S., Wang, D., Huang, L., Zhang, Y., Luo, R., Adah, D., et al. (2019). The complement receptor C5aR2 promotes protein kinase R expression and contributes to NLRP3 inflammasome activation and HMGB1 release from macrophages. *The Journal of Biological Chemistry, 294*, 8384–8394.
7. Ren, G., Zhang, X., Xiao, Y., Zhang, W., Wang, Y., Ma, W., et al. (2019). ABRO1 promotes NLRP3 inflammasome activation through regulation of NLRP3 deubiquitination. *The EMBO Journal*. https://doi.org/10.15252/embj.2018100376.
8. Baroja-Mazo, A., Martin-Sanchez, F., Gomez, A. I., Martinez, C. M., Amores-Iniesta, J., Compan, V., et al. (2014). The NLRP3 inflammasome is released as a particulate danger signal that amplifies the inflammatory response. *Nature Immunology, 15*, 738–748.
9. Liu, D., Zeng, X., Li, X., Mehta, J. L., & Wang, X. (2018). Role of NLRP3 inflammasome in the pathogenesis of cardiovascular diseases. *Basic Research in Cardiology, 113*, 5.
10. Minutoli, L., Puzzolo, D., Rinaldi, M., Irrera, N., Marini, H., Arcoraci, V., et al. (2016). ROS-Mediated NLRP3 Inflammasome activation in brain, heart, kidney, and testis ischemia/reperfusion Injury. *Oxidative Medicine and Cellular Longevity, 2016*, 2183026.
11. Jin, Y., & Fu, J. (2019). Novel insights into the NLRP 3 inflammasome in atherosclerosis. *Journal of the American Heart Association, 8*, e012219.
12. Luo, B., Huang, F., Liu, Y., Liang, Y., Wei, Z., Ke, H., et al. (2017). NLRP3 Inflammasome as a molecular marker in diabetic cardiomyopathy. *Frontiers in Physiology, 8*, 519.
13. Abais, J. M., Xia, M., Zhang, Y., Boini, K. M., & Li, P. L. (2015). Redox regulation of NLRP3 inflammasomes: ROS as trigger or effector? *Antioxidants & Redox Signaling, 22*, 1111–1129.
14. Songbo, M., Lang, H., Xinyong, C., Bin, X., Ping, Z., & Liang, S. (2019). Oxidative stress injury in doxorubicin-induced cardiotoxicity. *Toxicology Letters, 307*, 41–48.
15. Li, W., Zhang, Z., Li, X., Cai, J., Li, D., Du, J., et al. (2019). CGRP derived from cardiac fibroblasts is an endogenous suppressor of cardiac fibrosis. *Cardiovascular Research*. https://doi.org/10.1093/cvr/cvz234.
16. Li, W. Q., Li, X. H., Wu, Y. H., Du, J., Wang, A. P., Li, D., et al. (2016). Role of eukaryotic translation initiation factors 3a in hypoxia-induced right ventricular remodeling of rats. *Life Sciences, 144*, 61–68.
17. Wei, S., Sun, T., Du, J., Zhang, B., Xiang, D., & Li, W. (2018). Xanthohumol, a prenylated flavonoid from Hops, exerts anticancer effects against gastric cancer in vitro. *Oncology Reports, 40*, 3213–3222.
18. Chen, G. Y., & Nunez, G. (2010). Sterile inflammation: Sensing and reacting to damage. *Nature Reviews Immunology, 10*, 826–837.
19. Latz, E., Xiao, T. S., & Stutz, A. (2013). Activation and regulation of the inflammasomes. *Nature Reviews Immunology, 13*, 397–411.
20. Mezzaroma, E., Toldo, S., Farkas, D., Seropian, I. M., Van Tassell, B. W., Salloum, F. N., et al. (2011). The inflammasome promotes adverse cardiac remodeling following acute myocardial infarction in the mouse. *Proceedings of the National Academy of Sciences of the United States of America, 108*, 19725–19730.
21. Kawaguchi, M., Takahashi, M., Hata, T., Kashima, Y., Usui, F., Morimoto, H., et al. (2011). Inflammasome activation of cardiac fibroblasts is essential for myocardial ischemia/reperfusion injury. *Circulation, 123*, 594–604.
22. Lou, H., Danelisen, I., & Singal, P. K. (2005). Involvement of mitogen-activated protein kinases in adriamycin-induced cardiomyopathy. *American Journal of Physiology Heart and Circulatory Physiology, 288*, H1925–1930.
23. Maier, H. J., Schips, T. G., Wietelmann, A., Kruger, M., Brunner, C., Sauter, M., et al. (2012). Cardiomyocyte-specific IkappaB kinase (IKK)/NF-kappaB activation induces reversible inflammatory cardiomyopathy and heart failure. *Proceedings of the National Academy of Sciences of the United States of America, 109*, 11794–11799.
24. De Luca, G., Cavalli, G., Campochiaro, C., Tresoldi, M., & Dagna, L. (2018). Myocarditis: An Interleukin-1-mediated disease? *Frontiers in Immunology, 9*, 1335.
25. Kraft, L., Erdenesukh, T., Sauter, M., Tschope, C., & Klingel, K. (2019). Blocking the IL-1beta signalling pathway prevents chronic viral myocarditis and cardiac remodeling. *Basic Research in Cardiology, 114*, 11.

26. Sho, T., & Xu, J. (2019). Role and mechanism of ROS scavengers in alleviating NLRP3-mediated inflammation. *Biotechnology and Applied Biochemistry, 66*, 4–13.
27. Goffart, S., von Kleist-Retzow, J. C., & Wiesner, R. J. (2004). Regulation of mitochondrial proliferation in the heart: Power-plant failure contributes to cardiac failure in hypertrophy. *Cardiovascular Research, 64*, 198–207.
28. Tang, Y. S., Zhao, Y. H., Zhong, Y., Li, X. Z., Pu, J. X., Luo, Y. C., et al. (2019). Neferine inhibits LPS-ATP-induced endothelial cell pyroptosis via regulation of ROS/NLRP3/Caspase-1 signaling pathway. *Inflammation Research, 68*, 727.
29. Xu, M., Wang, L., Wang, M., Wang, H., Zhang, H., Chen, Y., et al. (2019). Mitochondrial ROS and NLRP3 inflammasome in acute ozone-induced murine model of airway inflammation and bronchial hyperresponsiveness. *Free Radical Research, 53*, 1–11.
30. Li, W., He, W., Xia, P., Sun, W., Shi, M., Zhou, Y., et al. (2019). Total extracts of *Abelmoschus manihot* L. attenuates adriamycin-induced renal tubule injury via suppression of ROS-ERK1/2-mediated NLRP3 inflammasome activation. *Frontiers in Pharmacology, 10*, 567.